Contents lists available at http://qu.edu.iq

Al-Qadisiyah Journal for Engineering Sciences

Journal homepage: https://qjes.qu.edu.iq

Numerical analysis of one-way continuous slab with partial corrosion strengthened with different material

Ammar K. AL-Najar * ***and Labeeb S. AL-Yassri***

Department of Civil Engineering, College of Engineering, University of Al-Qadisiyah, Iraq.

ARTICLE INFO

Article history:
Received 10 November 2020
Received in revised form 11 December 2020
Accepted 15 January 2021

Keywords:
Numerical Analysis
Corrosion
Construction joint
Negative reinforcement
CFRP
NSM
Steel plate

ABSTRACT

This paper investigates numerically the combined effects of a construction joint and reduction in the cross-section area of negative reinforcement in a one-way continuous slab on the structural behavior and the efficiency of three types of strengthening techniques. In this paper, the models made by ABAQUS (software) are used to numerically represent the specimens and simulate the applied loading. This numerical study's models represent six one-way continuous slabs, as a part of an experimental study. The specimen's dimensions were (2200 mm in length, 500 mm in width, and 100 mm in thickness). Five of the six models had a vertical construction joint and reduced the negative reinforcement steel bars' cross-sectional area. The sixth specimen is used as a reference. The proposed strengthening technique was Carbon fiber Reinforced Polymers strips, 6 mm Carbon fiber Reinforced Polymers bars Near the Surface Mountain technique, and steel plates. All the proposed strengthening's applied to the tension side on the top face at the internal support. The program outcomes are represented visually as stress distribution diagrams, load-deflection curves, and crack patterns. The results from the numerical analysis compared to the experiment results. In the experiment, the reduction in the cross-section area resulting from partial corrosion happened in one span due to the outdoor atmosphere's exposure because of the stoppage in the concrete pouring, which also resulted in forming the construction joint. The results highlighted the construction joint's effect and the steel cross-sectional area reduction on the ultimate load and the deflection. The proposed strengthening methods improved the member's overall responses, and There was a good convergence between the numerical and experimental works that verify the specimens' observed behavior.

1. Introduction

Buildings and bridges need rehabilitation or strengthening for different causes. The composite materials strengthen different structural members such as beams, slabs, and masonry walls Meier [1]. A study conducted by Elsanadedy et al.[2] to analyze by using the finite element method of FRP utilization to enhance the one-way slab flexural strengthening. Eight specimens were used. Two are considered as a reference without strengthening. Two samples were strengthened with five CFRP strips (50 mm width and 1080 mm length). Two specimens were strengthened with five (200 mm width and 1080 mm long) CFRP strips, and the last two samples were strengthened with five GFRP strips (200 mm width and 1080 mm long). All strengthening externally bonded to the tension face. The LS-DYNA was a computer software used to execute the analysis. The

* *Corresponding author.*
E-mail address: amarkreem24@gmail.com(Ammar K. AL-Najar)

https://doi.org/10.30772/qjes.v14i1.713

research came up with the conclusion that the model was suitable to simulate the experimental work. According to the comparison between the numerical and experimental results, the model can further investigate other parameters. Foret and Limam [3] numerically analyzed four specimens of two-way reinforced concrete slabs to examine the efficiency of strengthening them with CFRP NSM bars and CFRP sheets to increase their flexural strength. The strengthening was 8 mm CFRP bars and 50 mm width CFRP sheets. A composite orthotropic plate model with a 2D finite element was created by the researcher to simulate the specimen's elastic behavior. After the numerical linear model was executed, a comparison between the experimental and the numerical results was made.

According to the results, there was an excellent convergence between the experimental and numerical work. The model was reliable. Bouguerra et al. [6] studied experimentally and numerically using FRP to rehabilitate the damaged bridge deck slab due to corrosion. A 35 MPa concrete was used to cast a 2500 mm square slab with 175 mm thickness subjected to point load in the middle in the experimental part. The numerical part was modeled on the slab with the FE model by ADINA 8.4 software. The study found a remarkable convergence regarding ultimate load and deflection between the experimental and numerical work. L-Yassri et al. [9] experimented with using hybrid reinforcement in hollow-core concrete slabs in the structure behavior. The main parameter was replacing conventional reinforcement with CFRP bars with a percentage of replacement (0, 50, and 100%). The study concluded that using CFRP bars with a steel bar was more effective than using only CFRP bars, and the shear capacity was slightly influenced by using the CFRP bars, while there was a decrease in the stiffness of specimens. Ranjitham and Manjunath [11] numerically investigated the use of bubble deck slabs as a replacement for conventional kinds of slabs. The model was greeted and analyzed by ANSYS. The numerical result is compared with the experimental result in regarding stress and deformation. the study found that both numerical and experimental models showed higher load-bearing capacity. There was an improvement in the slab behaviour in regard to deflection and weight parameter.

This paper adopts experiment results and structural details of a study conducted by Al-Najar and AL-Yassri [12]. A comparison between the numerical results and the adopted experiment was made. The experimental specimens of the adopted study consist of Six one-way continuous slabs. Those slabs were tested under a two-point monotonic load until complete failure-the specimens were cast with concrete, with an average 28-day compressive strength equal to (32.1 MPa). Specimen dimensions and reinforcement details are illustrated in Fig. 1 Five of six specimens had a vertical construction joint at the internal support and negative reinforcement loss in one span due to corrosion, while the sixth was without construction joint and steel losses. The steel losses of negative reinforcement, are illustrated in Table 4. In the experimental study, three types of strengthening suggested compensating for a construction joint's presence and the steel area losses. They were: two of 50 mm width of CFRP strips, two of 6 mm diameter CFRP bars applied with NSM technique, and two of 50 mm width and 5 mm thickness of steel plates. All proposed strengthening was applied to the tension face at internal support and extended in the two spans with a =L/3=350 mm aligned with the continuity axis of the specimens

Table 1. Specimens Classification

Specimens Symbols	Corrosion and Construction Joint	Strengthening
S-O-1	-------	----None--
S-O-2 (reference)	Partial corrosion in the Negative Reinforcement and Joint	----None ---
S-O-3 (reference)	Partial corrosion in the Negative Reinforcement and Joint	----None---
S-O-4	Partial corrosion in the Negative Reinforcement and Joint	Strengthened with CFRP Strips
S-O-5	Partial corrosion in the Negative Reinforcement and Joint	Strengthened with CFRP 6 mm bars NSM
S-O-6	Partial corrosion in the Negative Reinforcement and Joint	Strengthened with Steel Plates

2. Numerical analysis modeling

2.1. Parts, Properties, and Assembly

ABAQUS [13] is the finite element analysis program used to create the model representing the experimental study's specimen. The model creation process required drawing the specimens' components using the software's toolbars, concrete, reinforcements, and the strengthening, loading, and supporting parts with their dimensions and exact location. Material properties, either elastic or inelastic, gained from the control test assigned to the model's parts after drawing them.

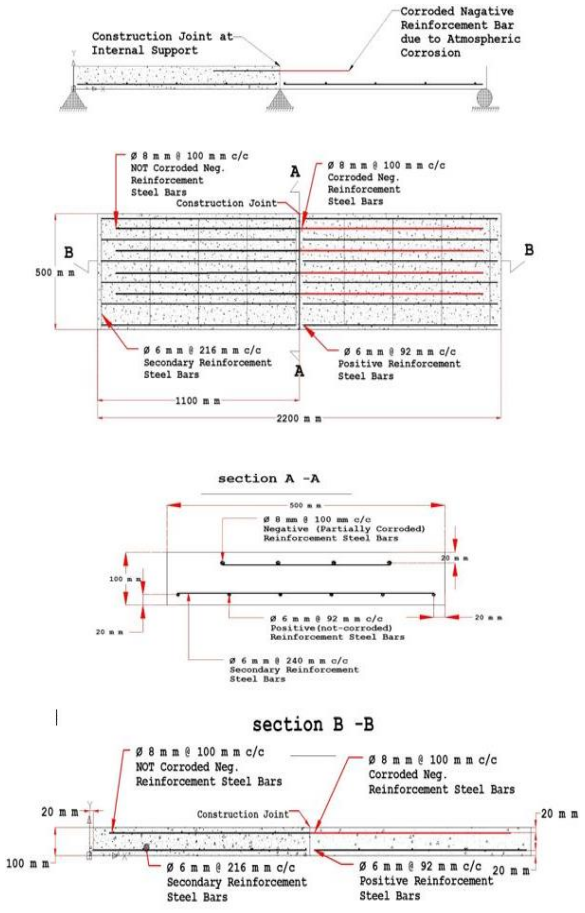

Figure 1. Specimens Dimension and Reinforcement Details [12]

To make the numerical analysis represent the specimen's actual structural behavior, the model should be as far as possible identical to the experimental specimens regarding material properties dimensions and loading conditions. All specimen parts resembled in Fig. 2), and the losses in steel bars due to partial corrosion are represented in the numerical study by reducing the bar diameter, as shown in Fig. 3.

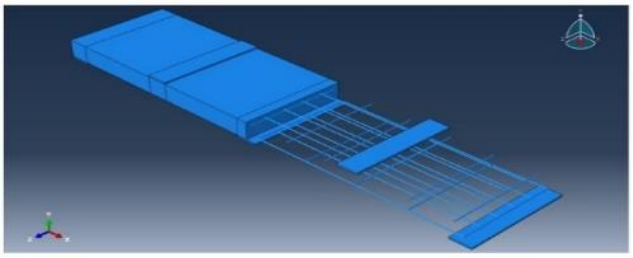

Figure 2. Parts and assembly

Figure 3. Change in the bar diameter due to corrosion

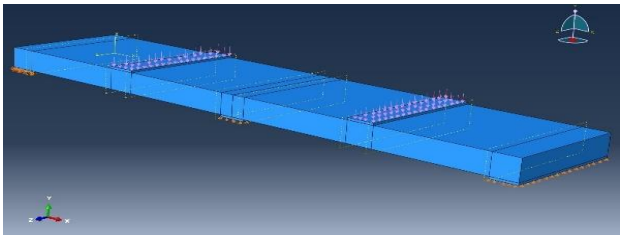

Figure 3: Loading and boundary conditions

2.2. Interaction between the parts

To model a composite member and after drawing each element separately and giving each one a proper section, it was necessary to connect the parts by assigning the suitable connect type. (See Table 2).

Table 2. Contact between the different parts

Parts	Type of Interaction
Concrete-steel bars	Embedded
Concrete-loading plate	Rigid body
Concrete-CFRP bars	Embed
Concrete-steel plate	Surface-to-surface (cohesive)
Concrete-CFRP strips	Surface-to-surface (cohesive)
Old Concrete-New concrete	Surface-to-surface (cohesive)

2.3. Finite element modeling

Concrete, loading plate, support, and other parts were modeled in the finite element program (see Table 2). The concrete elements were modeled using (T3D2) 3D 8 nodes bricks elements to gain sufficient distribution of stress while the steel bars meshed to linear truss elements (2 nodes elements) [14, 15]. Depending on the convergence study for mesh, a 35 mm mesh size is adopted.

Table 3. Finite element modeling

Part	Element Type (three degrees of freedom for each node)
Concrete	Linear hexahedron, type C3D8 (8 nodes)
Support	Linear hexahedron, type C3D8(8 node)
Loading Plate	Linear hexahedron, type C3D8(8 node)
Steel Bars	Linear line, type T3D2(2 node)
CFRP Bars	Linear line, type T3D2(2 node)
Steel Plate	Linear hexahedron, type C3D8(8 node)
CFRP Strips	Linear quadrilateral, type S4R(4 node)

2.4. Loading and boundary conditions

The loading plates were square steel plates 100 mm and 100mm wide placed at mid-distance between supports and extended along slab width. The Load in ABAQUS presented as uniform pressure after. Boundary conditions were applied at supports (10 mm thickness), which were three paces in the experiment. The first support was in the begging, the second in the middle, and the third was in the end. The displacement was constrained for the first support in three directions X, Y, and Z, while the other two were in one direction Y, the rotation was allowed in the three supports (see Fig. 4).

2.5. Analytic results

After completing all requirements and all the needed data to run the simulation, the program analyzes. The result was interpreted visually by the load-deflection curve and deformed shape. According to the changes in parameters (corrosion percentage and the strengthening methods), the ultimate load and deflection will also vary. The convergence between the numerical and experimental results indicated the reliability of the model. Tables 4 and 5 show the ultimate load, deflection, and failure mode experientially and numerically. Figures 5 to 9 show a load-deflection curve for each specimen. In experimental and numerical analysis, the same symbolic schema was adopted. In the (S-O-X) symbol, the "S" refers to the member type, which is a slab, the "O" refers to the type of slab which was a one-way slab, and the "X" is a variable ranging between 1 to 6 (see Table 3).

Table 4. Experimental and numerical ultimate load

Specimen	Losses in Steel Area %	Ultimate load (kN)	
		Exp.[12]	Num.
S-O-1	0.00%	110	111
S-O-2andS-O-3	51.57%	75	78.8
S-O-4	54.30%	116	122
S-O-5	48.92%	117	114
S-O-6	0.4517	112	109.6

Table 5. Experimental and numerical deflection at ultimate load and failure mode

Specimen	Deflection at Ultimate Load (mm)		Failure Mode	
	Exp.	Num.	Exp.	Num.
S-O-1	11.7	7.3	Flexural Tensile Failure	Flexural Tensile Failure
S-O-2and S-O-3	4.3	4.4	Flexural Tensile Failure	Flexural Tensile Failure
S-O-4	9.7	9.8	De-Bond of CFRP Strips Followed by Flexural Tensile Failure	De-Bond of CFRP Strips Followed by Flexural Tensile Failure
S-O-5	12.1	10	De-Bond of CFRP bars Followed by Flexural Tensile Failure	De-Bond of CFRP bars Followed by Flexural Tensile Failure
S-O-6	13.2	11	De-Bond of Steel Plates Followed by Flexural Tensile Failure	De-Bond of Steel Plates Followed by Flexural Tensile Failure

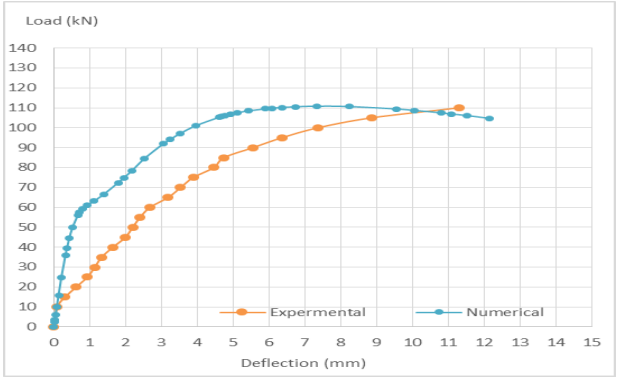

Figure 5. Experimental and Numerical Load-Deflection Curves for S-O-1 Specimen

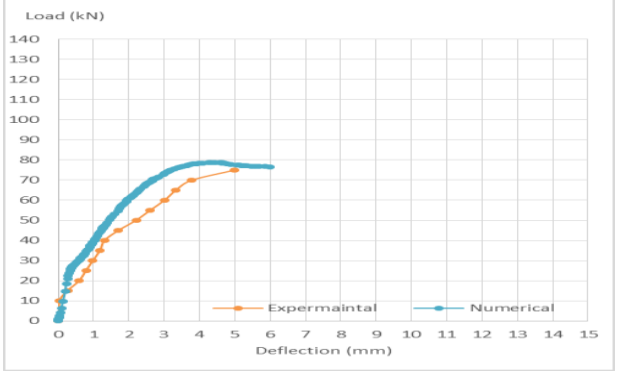

Figure 4. Experimental and Numerical Load-Deflection Curves for S-O-2 and S-O-3 Specimens

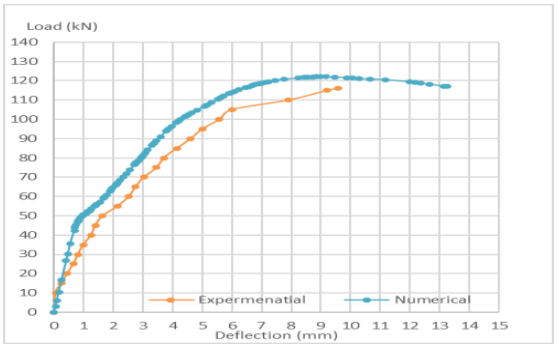

Figure 5. Experimental and Numerical Load-Deflection Curves for S-O-4 specimen

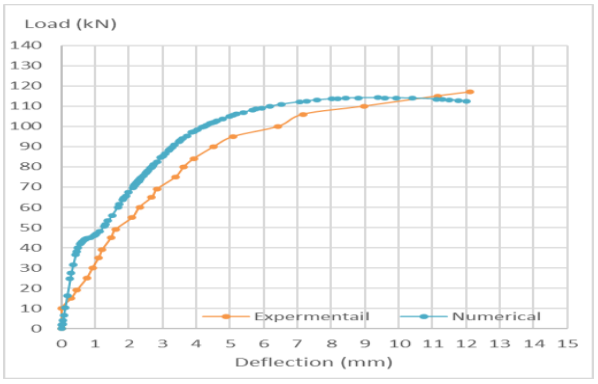

Figure 6. Experimental and Numerical Load-Deflection Curves for S-O-5 Specimen

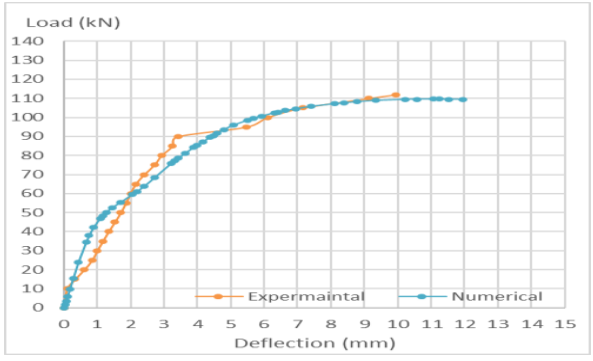

Figure 7. Experimental and Numerical Load-Deflection Curves for S-O-6

2.6. Cracks pattern

According to observations from the experimental test, the tension cracks in one-way slabs were perpendicular to the slab axis, also concentrated in the bottom face and extended to slabs sides in addition to the tension zone of the negative moment at the internal support, which results in the opening of the joint. The analytical part showed that the damaged tension areas, which can develop into cracks, were identical to the experimental work.

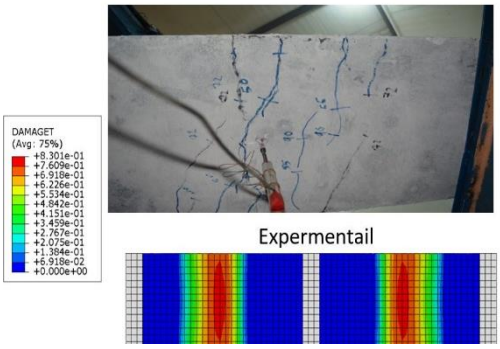

Figure 8. Experimental and numerical cracks pattern of S-O-1 specimen

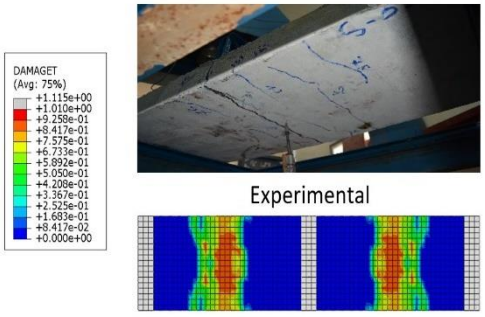

Figure 9. Experimental and numerical cracks pattern of S-O-3 specimens

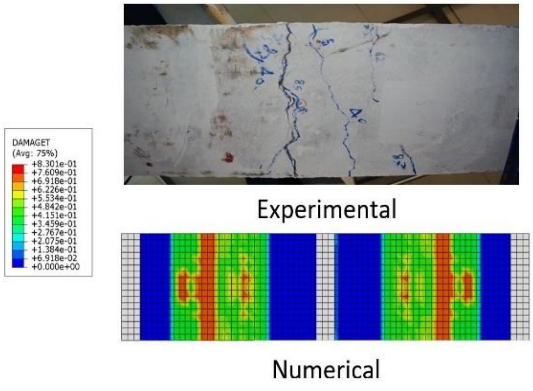

Figure 10. Experimental and numerical cracks pattern of S-O-4 specimen

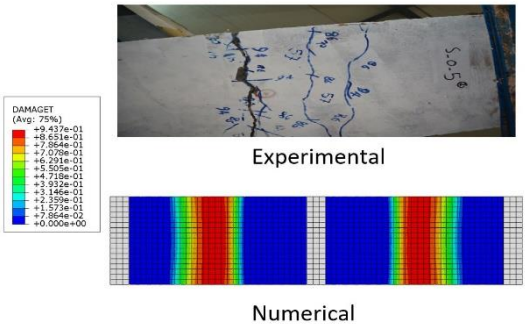

Figure 11. Experimental and numerical cracks pattern of S-O-5 specimen

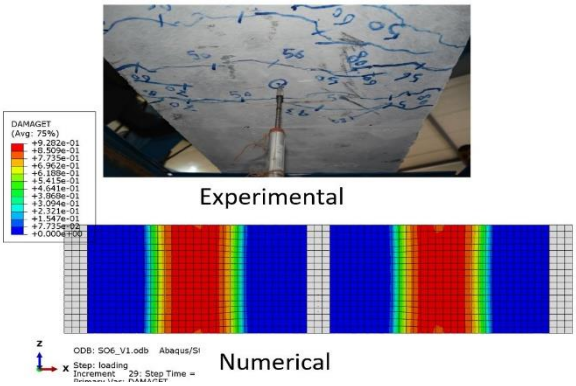

Figure 12. Experimental and numerical cracks pattern of S-O-6 specimen

2.7. Failure Mode

The experiment specimens failure mode was similar: the strengthening debond from concrete followed by flexural failure for strengthened specimens. It was a flexural failure for the not strengthened specimens. In the numerical study, the tension damage areas (which indicate the failure) spread similarly to the experimental (see Figures 15 to 19).

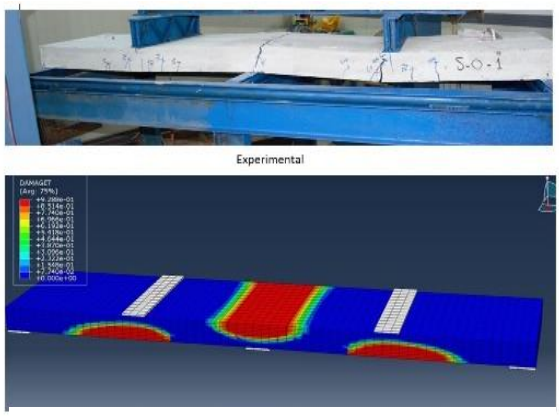

Figure 13. Failure mode of S-O-1 specimen

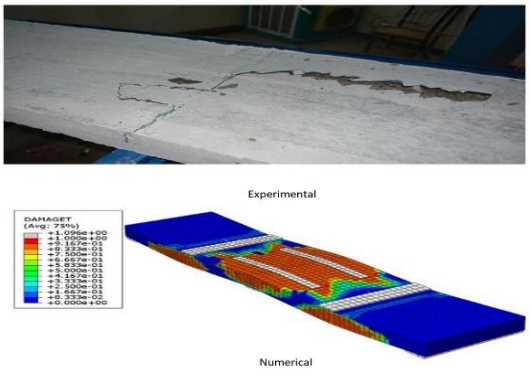

Figure 15. Failure mode of S-O-4 specimen

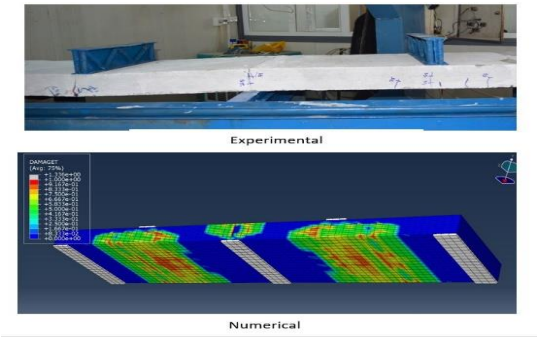

Figure 14. Failure mode of S-O-2 and S-O-3 specimens

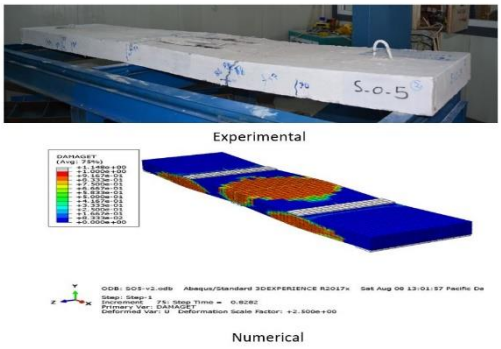

Figure 16. Failure mode of S-O-5 specimen

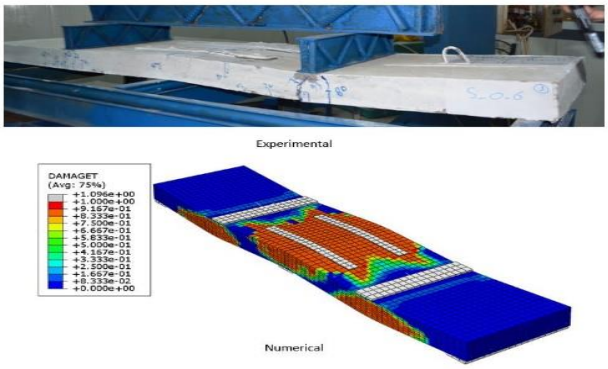

Figure 17: Failure mode of S-O-6 specimen

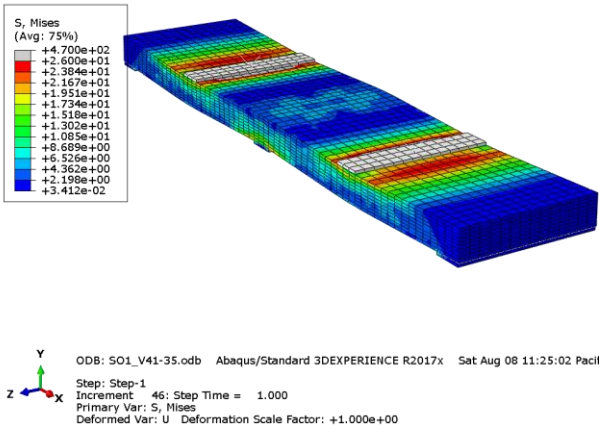

Figure 18. Mises stresses in S-O-1 specimen

2.8. ises Stresses (Von Mises Theory)

The failure is happening when the material was subjected to increasing in load, which leads eventually to fail or is a state that prevents the structure from the purpose which builds for it. Failure, in general, can be defined as Fracture with very little yielding, permanent deformation. Fracture is one of many modes for failure: a separation of the object for two or more parts by a brittle or ductile mechanism.

From the Figures (20 to 24), it becomes evident that the strengthening method and losses in steel have been influenced by the distribution of stresses. The areas surrounding the loading plates show higher stresses, and this is similar to the experimental work.

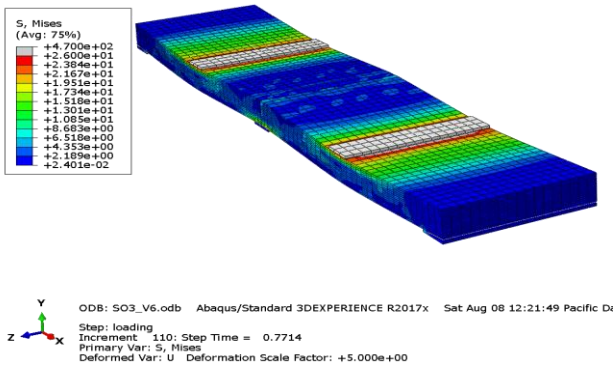

Figure 19. Mises stresses in S-O-2 and S-O-3specimenS

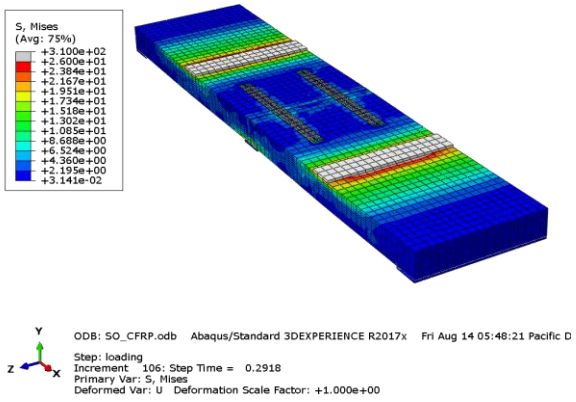

Figure 20. Mises stresses in S-O-4 specimen

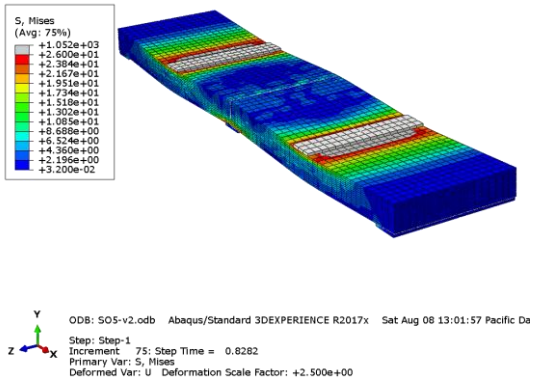

Figure 21. Mises stresses in S-O-5 specimen

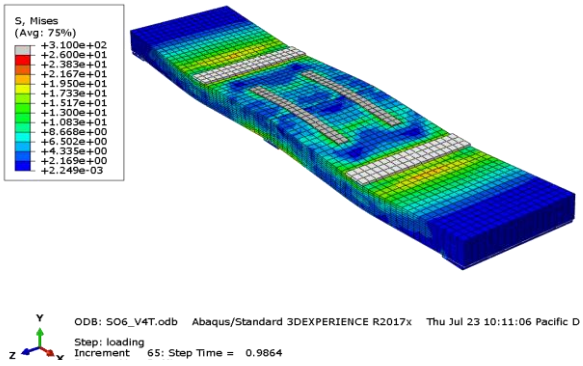

Figure 22. Mises stresses in S-O-6 specimen

3. Parametric study

In each experimental work, increasing the targeted parameter will increase the work complexity and lead to the result's interference, making it hard to connect the unique variables to its influence. Since we found that the model is reliable in this study will test the influence of changing variable and its influence on the model, which reflects approximately the actual behavior. The one-way slabs (S-O-3) chosen to investigate the difference that could be happening if the compressive strength increased to 40,50,60,70 MPa (see **Fig. 25**)

Table 6. Parametric study results

fc (MPa)	Pu (kN)	Δ_u (mm)	$(Pu^{**} - Pu^{*})/Pu^{*}$ (%)	$(\Delta_u{}^{**} - (\Delta_u{}^{*})/(\Delta_u{}^{***}$ (%)
32	78.8	4.42	--------	--------
40	80	4.20	1.52	-4.84163
50	80.3	4.25	1.9	-3.84615
60	80.8	4.37	2.54	-1.13122
70	81.8	4.38	3.81	-0.90498

$Pu^{*} = 32\ (MPa)$
$Pu^{**} = Pu_{fc(40-70)}\ (MPa)$
$\Delta_u{}^{*} = 4.42(mm)$
$\Delta_u{}^{**} = \Delta_{fc(40-70)}(mm)$

Increasing the compressive strength will increase the ultimate load and reduce the deflection. Still, this increase will not compensate for reducing the corrosion and the construction joint's presence.

4. Conclusions

1) A good convergence regarding the ultimate load, deflection, and failure mode were between the numerical and experimental works.
2) ABAQUS's created model predicted to an acceptable degree the structural behavior of a member and highlighted the potential failure regions with high accuracy.
3) According to the gained results from the numerical analysis found that the model was reliable and could implement with confidence.
4) The numerical analysis found that reducing the cross-section area of steel bars and construction joints led to a reduction in the ultimate capacity compared to the not corroded specimen (28.8%). The experiment was (31.8%).

5) According to the parameter study, increasing the compressive strength of used concrete will increase the load capacity and reduce the deflection.

Authors' contribution

All authors contributed equally to the preparation of this article.

Declaration of competing interest

The authors declare no conflicts of interest.

Funding source

This study didn't receive any specific funds.

REFERENCES

[1] U. Meier, "Bridge repair with high performance composite materials," no. January 1987, 2019.

[2] H. M. Elsanadedy, T. H. Almusallam, S. H. Alsayed, and Y. A. Al-salloum, "Experimental and FE Study on RC One-Way Slabs Upgraded with FRP Composites," vol. 00, no. 0000, pp. 1–17, 2014, doi: 10.1007/s12205-013-0689-y.

[3] G. Foret and O. Limam, "Experimental and numerical analysis of RC two-way slabs strengthened with NSM CFRP rods," Constr. Build. Mater., vol. 22, no. 10, pp. 2025–2030, 2008, doi: 10.1016/j.conbuildmat.2007.07.027.

[4] M. Lucia and H. Jaroslav, "Numerical Analysis of the Experimental Flat Slabs," vol. 292, pp. 134–139, 2019, doi: 10.4028/www.scientific.net/SSP.292.134.

[5] B. Kuriakose, "Numerical Analysis of One-way RC Slabs Subjected to Air Blast Loading," no. June 2016, 2017, doi: 10.3850/9789810962784-1570150411.

[6] K. Bouguerra, H. Tobbi, and B. Benmokrane, "EXPERIMENTAL AND NUMERICAL INVESTIGATIONS OF FRP - REINFORCED BRIDGE DECK SLABS," no. December, 2019.

[7] A. Mohammed, "Numerical Investigation on the Influence of Web Opening on the Structural Behaviour of RC Deep Beams," vol. 12, pp. 178–183, 2019.

[8] N. Hussien and H. Al-thairy, "Numerical Study on the Performance of GFRP RC Beams Exposed to High Temperature," vol. 13, pp. 136–143, 2020.

[9] L. S. Al-Yassri, E. Labeebhuseinqueduiq, A. Y. Ali, and M. M. Al-khafaji, "EXPERIMENTAL INVESTIGATION FOR THE BEHAVIOR OF HOLLOW CORE CONCRETE SLAB REINFORCED WITH," vol. 10, no. 3, pp. 308–317, 2017.

[10] A. S. Dheyab, C. Engineering, and C. Engineering, "Numerical Investigation of Structural Behavior Of Fiber Reinforced Polymers Filled Sandwich Panels," vol. 8, no. 3, pp. 10–18.

[11] M. Ranjitham and N. V Manjunath, "International Journal of Trend in Scientific Research and Development (IJTSRD) Experimental and numerical investigation on structural behaviour of Bubble Deck Slab with conventional slab," pp. 2614–2617, 2018.

[12] A. J. Al_Najar and L. S. AL-Yassri, "Structure behavior of continuous reinforced concrete member with corroded reinforcement at internal support strengthened CFRP," Al-Qadisiyah, 2020.

[13] C. A. E. User, "Abaqus 6.13."

[14] S. K. H. Al-Jasmi, "Behavior and Failuer Mode of Reinforced Concrete Beam with Lightweight Aggregate Subjected to Elevated Temperatuers," 2019.

[15] N. H. A. Al-hasnawi, "Behavior and Failure Modes of Reinforced Concrete Beams Strengthened by CFRP under Elevated Temperature," University of Al-Qadisiyah, 2020.

[16] J. Ye, Structural and Stress Analysis. Taylor & Francis, 2008.